Longitudinal Bunch Profile Measurements Using WCM and Streak Camera Techniques

Kurt Hahn[*]
Rochester Institute of Technology
Rochester, NY, USA
10.08.2025

Abstract
Reliable and precise longitudinal bunch profile measurements are essential for maintaining high-quality beams across the CERN accelerator complex. In the Super Proton Synchrotron (SPS), the longitudinal beam observation system utilizes a Wall Current Monitor (WCM) to measure the beam profile signal and is acquired by an oscilloscope operating at up to 40 GS/s. However, distortions caused by cabling, electronics, and attenuation between the beam pick-up and the oscilloscope affect the measured profile, requiring compensation based on the transfer function of the system. Alternatively, a streak camera system, used for the AWAKE experiment after extraction from the SPS, offers temporal resolution on the order of a few picoseconds with minimal signal distortion. This work presents the comparison between the bunch profile measured with the WCM in the SPS and the streak camera. The results, based on two different measurement techniques, will be processed and compared to assess precision and accuracy.

1 Introduction

The Super Proton Synchrotron (SPS) is the largest injector of the CERN accelerator complex with a circumference of almost seven kilometers. It delivers various types of particle beams to multiple experiments, including AWAKE (Advanced WAKefield Experiment). AWAKE's goal is to accelerate electrons using plasma wakefields generated by the passage of a very dense proton bunch with a width of less than one nanosecond [1].

In the longitudinal plane, ensuring high-quality beams in an accelerator relies on precise and reliable bunch profile measurements. In addition, beam stabilization mechanisms, such as Landau damping, are very sensitive to the bunch length [2].

In the SPS, measurement of the longitudinal bunch profiles is performed with a coaxial pick-up wall current monitor (WCM). However, the measured signal is fed through several electronics, attenuators, and cabling, which distort the signal before it is read out by an oscilloscope operating at up to 40 GS/s with an 8-bit vertical resolution [3]. The distortion can be compensated a posteriori with the so-called transfer function of the system.

The AWAKE experiment uses a Streak Camera (SC) to measure bunch intensity profiles. It is based on a photocathode and fast electron sweeping to convert light from the proton bunch (via optical transition radiation) into a time-resolved image, enabling direct measurement of the proton line density. It offers picosecond resolution with minimal signal distortion compared to the WCM [4].

In this work, we introduce the two different techniques to characterize and compare the measured bunch profiles. In particular, due to background noise and residual distortion from the acquisition systems, different observables based on the bunch length at varying signal amplitudes are considered.

[*]CERN, SY-RF-BR Supervisors: Leandro Intelisano & Giulia Papotti

Finally, taking advantage of the low distortion of the SC signal, we estimate the transfer function of the WCM acquisition system by comparing, in the frequency domain, the outputs of both methods obtained from the same event.

2 Mathematical framework

2.1 Transfer function

Time-invariant linear systems, such as pick-ups or cabling, can be characterized by transfer functions. For such devices, an input signal can be distorted. To correct for these distortions, we must know the transfer function of the device $H[s]$ given by the equation

$$H[s] = \frac{Y[s]}{X[s]} = \frac{\mathcal{L}\{y[t]\}}{\mathcal{L}\{x[t]\}} \tag{1}$$

where $y[t]$ and $x[t]$ are the output and input signals in the time domain, respectively, and $Y[s]$ and $X[s]$ are the output and input signals in the complex frequency domain, respectively [5]. Given an output signal spectrum $Y[s]$ of a device of known transfer function $H[s]$, the true signal spectrum $X[s]$ may be obtained by

$$X[s] = \frac{Y[s]}{H[s]} \ . \tag{2}$$

The above operation is equivalent to a deconvolution of the transfer function in the time domain. In our experiment, the transfer function of the wall current monitor is known; more precisely, there is a known transfer function $H_{\text{Pickup}}[s]$ for the APWL pick-up system and a transfer function $H_{\text{Cable}}[s]$ for the Machine Developments (MD) transfer line that directs the signal from the WCM to the oscilloscope in the Faraday cage [5, 6]. The total transfer function of the WCM measurement system is the product

$$H[s] = H_{\text{Cable}}[s] H_{\text{Pickup}}[s] \ . \tag{3}$$

2.2 Raised-cosine frequency filter

In general, it is desirable to reduce or remove noise at specific frequencies from a signal. This involves taking a signal spectrum in the real frequency domain $X[\omega]$ and multiplying it by a frequency filter $\phi[\omega]$,

$$F[\omega] = \phi[\omega] X[\omega] \tag{4}$$

where $F[\omega]$ is the filtered profile in the frequency domain. In this project, we define our frequency filter function to be of the form

$$\phi[\omega] = \begin{cases} 1 & \omega \leq (1-\beta)\omega_0 \\ \frac{1}{2} + \frac{1}{2}\cos\left(\frac{\pi}{2\beta\omega_0}(|\omega| - (1-\beta)\omega_0)\right) & (1-\beta)\omega_0 < \omega \leq (1+\beta)\omega_0 \\ 0 & \text{otherwise} \end{cases} \qquad \omega, \omega_0 \geq 0, \ \ \beta \in [0, 1] \tag{5}$$

where ω_0 defines the center of the filter function in the frequency domain, and β determines the steepness of the filter, with $\beta = 0$ representing a hard cutoff at $\omega = \omega_0$.

2.3 Cross-correlation function

The cross-correlation function provides a measure of how well-aligned two signal profiles are as a function of the temporal displacement of one of the profiles. Given two profiles of the same length in the time domain, $x[t]$ and $y[t]$, the cross-correlation function $K[\tau]$ is given by

$$K[\tau] = \int_{-t_{\max}}^{t_{\max}} x[t]\, y[t+\tau]\, dt \tag{6}$$

where τ is the time lag, or displacement, of the second profile and $t_{\max}$ is the length of the signals. Suppose Δt is the time lag for which $K[t]$ is maximal. After displacing $y[t]$ along the time axis by Δt, the two profiles can be aligned.

2.4 Binomial distribution

Longitudinal bunch profiles can be assumed to have a binomial particle distribution, which is a distribution that covers most realistic profiles of proton bunches [2]. The distribution $B(t)$ is given by

$$B(t) = \begin{cases} \left(1 - 4\left(\frac{t-c}{\tau}\right)^2\right)^{\mu} & -\frac{\tau}{2} + c \leq t \leq \frac{\tau}{2} + c \\ 0 & \text{otherwise} \end{cases} \tag{7}$$

where c is the center of the profile in the time domain, τ is the bunch length, and μ is the tailform factor. For $\mu = 1$, the distribution becomes parabolic. As $\mu \to \infty$, the distribution becomes more Gaussian.

3 Longitudinal bunch profile measurement techniques and setup

3.1 APWL Wideband Wall Current Monitor

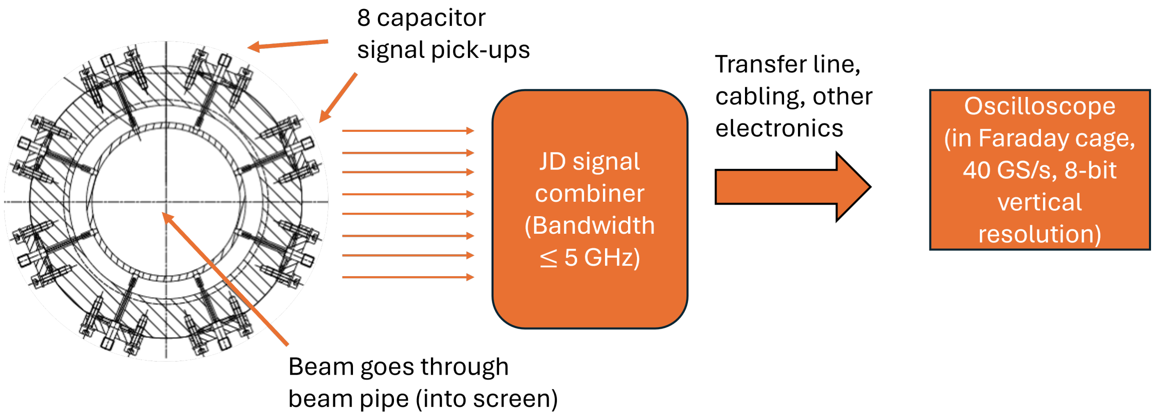

Figure 1: A schematic of the pick-up system of the WCM with the beam pipe directed through the page [3]. The beam pipe is surrounded by eight capacitor pick-ups that measure the voltage induced by the passing proton bunch. The signals are later combined in a JD combiner. The bandwidth of the pick-up system is reported to be 2.2 GHz. The combined signal is later sent through the MD transfer line up to the oscilloscope in the Faraday cage, which has a sampling rate of 40 GS/s and 8-bit vertical resolution.

The SPS currently employs a coaxial-type wall current monitor to measure bunch longitudinal profiles. A schematic of the pick-up system surrounding the beam pipe is given in Figure 1. Eight SubMiniature version A capacitor feedthroughs measure the induced voltage of the proton bunch as it passes through the beam pipe. The signals from each of these pick-ups are fed into a JD combiner, and the combined signal is then sent into the MD transfer line. A 2014 measurement of the pick-up and

MD line transfer functions is shown in Figures 2 and 3. Preliminary studies have reported a pick-up bandwidth of up to 2.2 GHz with the transfer function of the WCM system being well-behaved up to around 3 GHz [3].

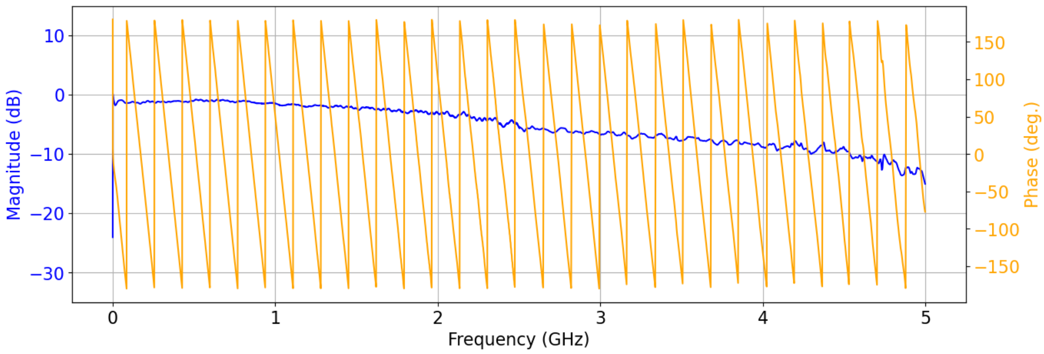

Figure 2: Normalized measured transfer function of the APWL pick-ups, as measured in 2006 [6]. In blue is the magnitude on a logarithmic scale, and in orange is the phase in degrees.

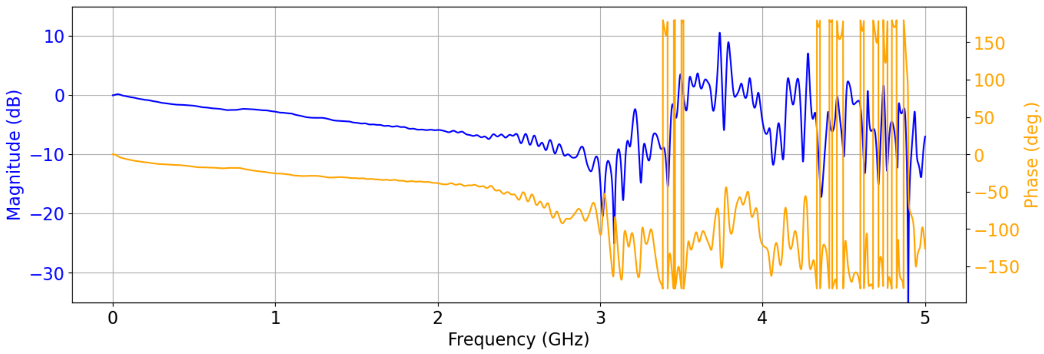

Figure 3: Normalized measured transfer function of the MD scope line for the WCM, as measured in 2014 [5]. In blue is the magnitude on a logarithmic scale, and in orange is the phase in degrees.

3.2 Hamamatsu Streak Camera C1090

Our second method of measuring bunch profiles is provided by the aforementioned AWAKE experiment, namely the Hamamatsu Streak Camera C1090 (SC) [4]. A schematic of the SC is provided in Figure 5. The operation of the SC involves the conversion of incident protons into photoelectrons. A time-dependent voltage deflects the photoelectrons onto a phosphorescent screen, producing an image representing the temporal (i.e., longitudinal) profile of the incident proton bunch. An example of such an image is depicted in Figure 4, where pixels towards the top of the image represent protons absorbed by the SC earlier in time, and pixels towards the bottom represent protons absorbed later in time. The pixel intensities of the digitized image are taken to be proportional to the proton bunch intensity.

3.3 Bunch rotation and extraction

The WCM is installed in the SPS as shown in Figure 6. In our experiments, we use single-bunch beams. For every turn of the proton bunch in the machine, we make a profile measurement using the WCM. After extraction from the SPS to the AWAKE experiment, the proton bunch is detected and absorbed by the SC. By adjusting the radio-frequency (RF) cavity voltage, we can control the longitudinal length of the proton bunch. To produce bunches with shorter longitudinal lengths, we initiate a bunch rotation in phase

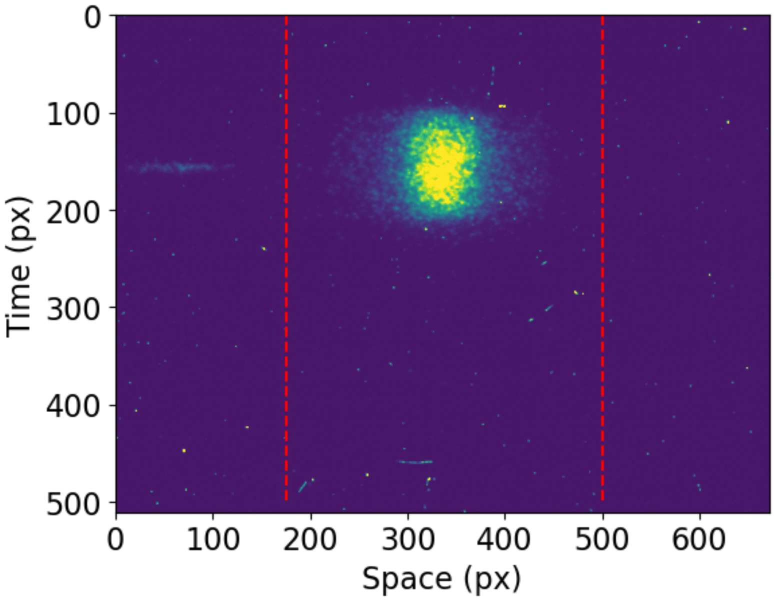

Figure 4: Measured image by the SC of a bunch from experiment B1. Pixels towards the top of the image represent protons that were detected earlier in time, and pixels towards the bottom, later in time. The region of interest is indicated between the dotted red lines.

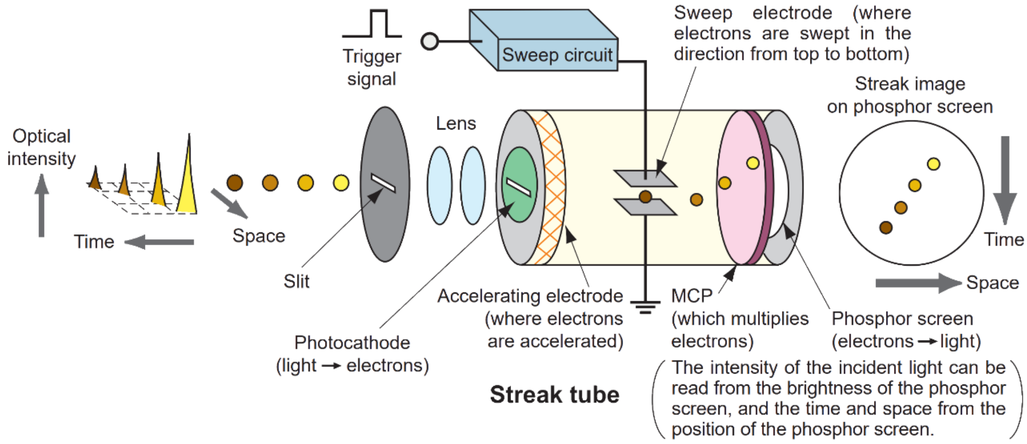

Figure 5: Schematic of the operation of the Hamamatsu Streak Camera C1090 used by the AWAKE experiment [7]. A proton bunch impinges on a scintillator foil (not shown), converting the proton beam signal into an optical signal. A photocathode then converts the optical signal into photoelectrons, and a trigger is sent to a sweep current connected to a capacitor. The sweep current produces a time-dependent voltage across the capacitor which deflects the photoelectrons as they pass through. This deflection is a function of time, where earlier photoelectrons are deflected up, and later ones, down. The signal is then multiplied in a microchannel plate before the photoelectrons are absorbed by a phosphor screen. The resulting phosphorescent image is then captured by a CMOS camera behind the screen (not shown).

Table 1: Parameters of each experiment showing the number of protons N_p, RF cavity voltage V, an approximate measurement of the bunch length τ_{approx}, whether or not the bunch is rotated in phase space, and the number of bunch measurements.

Experiment name	N_p	V	τ_{approx}	Bunch rotation	Number of acquisitions
A1	5×10^{10}	10 MV	0.80 ns	Yes	27
A2	10×10^{10}	10 MV	0.80 ns	Yes	30
A3	30×10^{10}	10 MV	0.80 ns	Yes	80
B1	3×10^{11}	10 MV	1.50 ns	No	5
B2	3×10^{11}	8 MV	1.70 ns	No	5
B3	3×10^{11}	6.5 MV	1.75 ns	No	5
B4	3×10^{11}	5 MV	1.90 ns	No	5
B5	3×10^{11}	3.5 MV	2.10 ns	No	5

space before extraction. We also control the number of protons within each bunch. Our acquisitions consist of measuring the longitudinal profile of multiple different single-bunches. The parameters of each experiment are tabulated in Table (1).

The longitudinal profile of the proton bunch was measured with the WCM and SC individually, and the data from each instrument was stored separately. To ensure that the acquired data of profile measurements were of the same bunch, it was necessary to check that the saved timestamps from each dataset were consistent within a few seconds. In some cases, the time discrepancy was much greater, so these measurements were discarded. In other cases, the SC did not have any image data, possibly because the bunch was dumped before extraction, so these measurements were discarded as well.

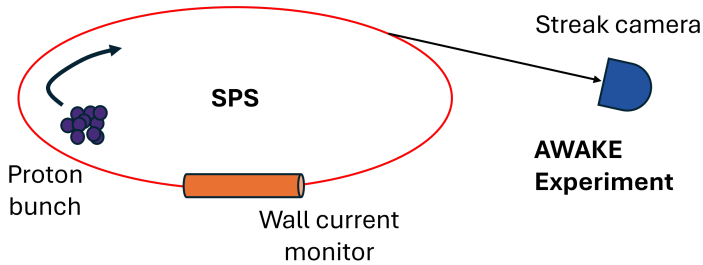

Figure 6: Schematic of the experimental setup in the SPS.

4 Data processing

4.1 Signal processing of wall current monitor data

The WCM measured the longitudinal bunch profile for 5000 turns in the SPS before bunch extraction. During this time, we controlled whether or not the bunch undergoes rotation in phase space. Figures 7 and 8 show all measured profiles of one bunch overlaid for experiment A1 with bunch rotation and experiment B1 without bunch rotation, respectively (see Table (1)).

To visualize the rotation and extraction of the bunch, we plot the maximum of each measured profile as a function of turn number, as shown in Figures 9 and 10. At a certain turn number, the maximum of the profile sharply goes to zero, indicating the extraction of the bunch. For the experiments with bunch rotation, we then obtain the measured profile of the bunch just before the extraction point. For experiments without bunch rotation, since the profile does not change appreciably as a function of turn number, we average the last twenty profiles before the extraction point, and we use the result as our measured profile.

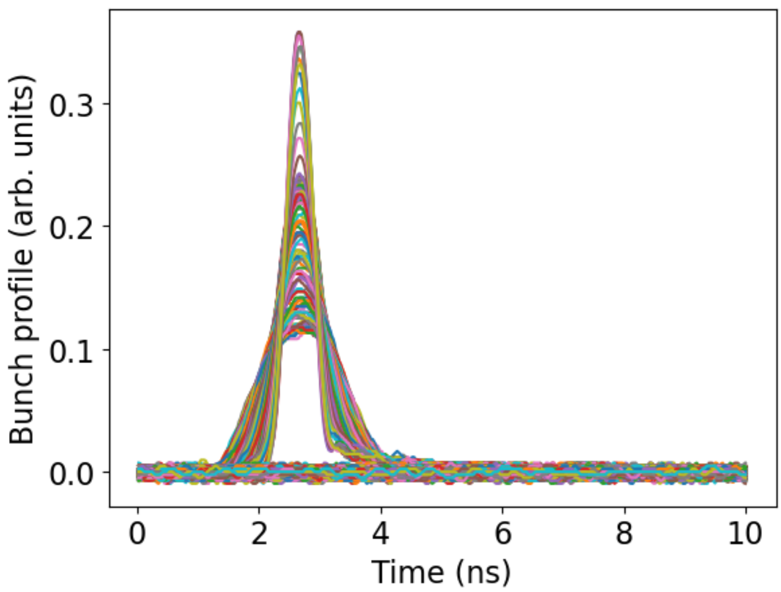

Figure 7: All measured profiles of the same bunch by the WCM for each turn with the experimental parameters listed in the A1 row of Table (1). Due to bunch rotation, the profile changes shape both in width and in amplitude.

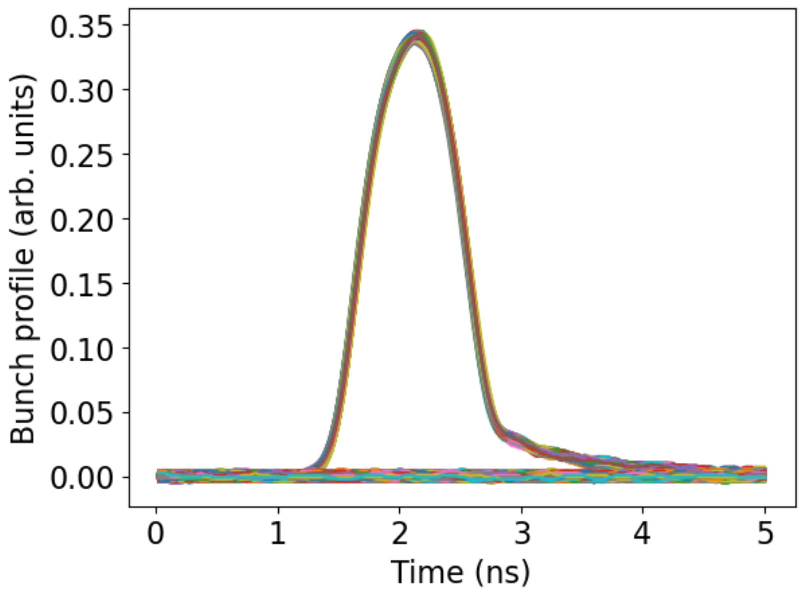

Figure 8: All measured profiles of the same bunch by the WCM for each turn with the experimental parameters listed in the B1 row of Table (1).

An example profile from a bunch in experiment B1 is shown in Figure 12. We then apply Equations (2) and (3) with the known transfer functions depicted in Figures 2 and 3 to obtain the corrected profile. We see that applying the inverse transfer functions removes the raised tail on the falling edge of the signal. Because the pick-up has a -3 dB bandwidth of 2.2 GHz, and the transfer function is well-behaved only up to 3 GHz, we apply a frequency filter as described by Equation (4). We use a raised-cosine function given by Equation (5) with parameters $\omega_0 = 2.5$ GHz and $\beta = 0.2$, which is depicted in Figure 11. The filter removes the ripples towards the ends of the profiles.

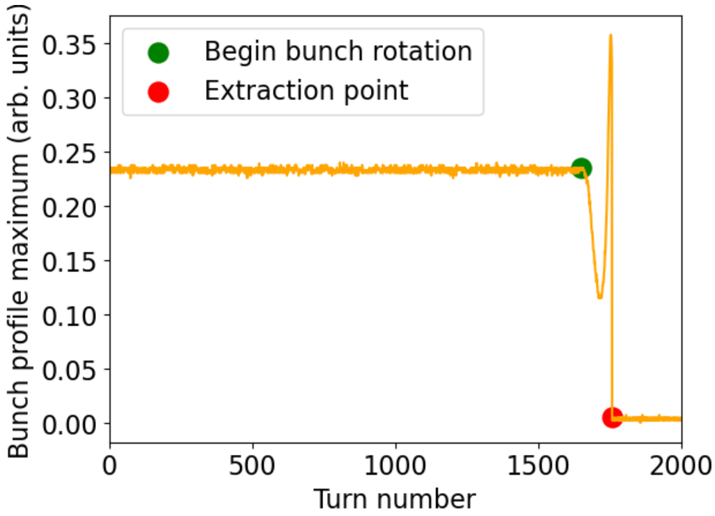

Figure 9: Profile maximum as a function of turn number for one bunch in experiment A1. At the green point around turn number 1600, we begin rotating the bunch in phase space resulting in profile peak that decreases before increasing again at around turn number 1750. The red point represents the extraction point, where the bunch is then sent to the SC at AWAKE.

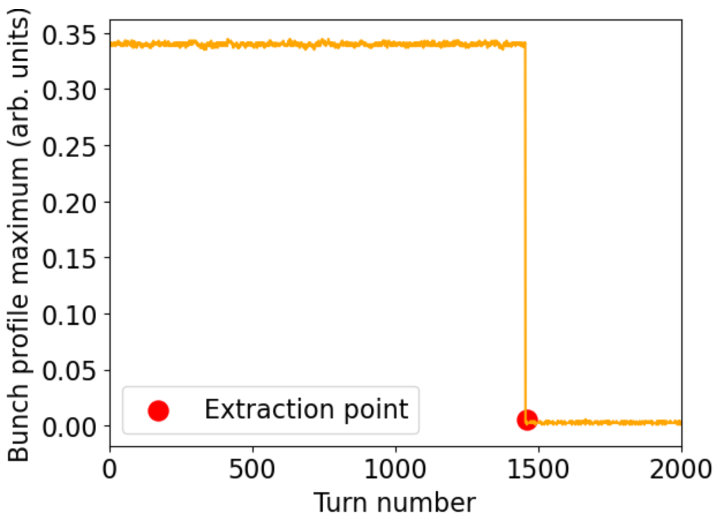

Figure 10: Profile maximum as a function of turn number for one bunch in experiment B1. The red point represents the extraction point, where the bunch is then sent to the SC at AWAKE.

4.2 Analysis of streak camera data

While the WCM can measure the longitudinal profile of a proton bunch for every turn in the SPS, the SC can only measure the profile once after extraction. The SC collects profile data in the form of images, as seen in Figure 4, which are 512 pixels in height and 672 pixels wide. To begin analysis, we crop the image to a 325-pixel wide region of interest centered on the bunch. In order to remove high-intensity pixel cluster noise, we then apply a median filtering algorithm with a kernel size of 5 pixels; the results are shown in Figure 13. This filtered image is then projected onto the time axis by summing all the pixel intensity values along the horizontal axis. After normalization, we then obtain the longitudinal profile of the bunch from the SC, as shown in Figure 14. For our comparisons, we then apply the same raised-cosine frequency filter depicted in Figure 11.

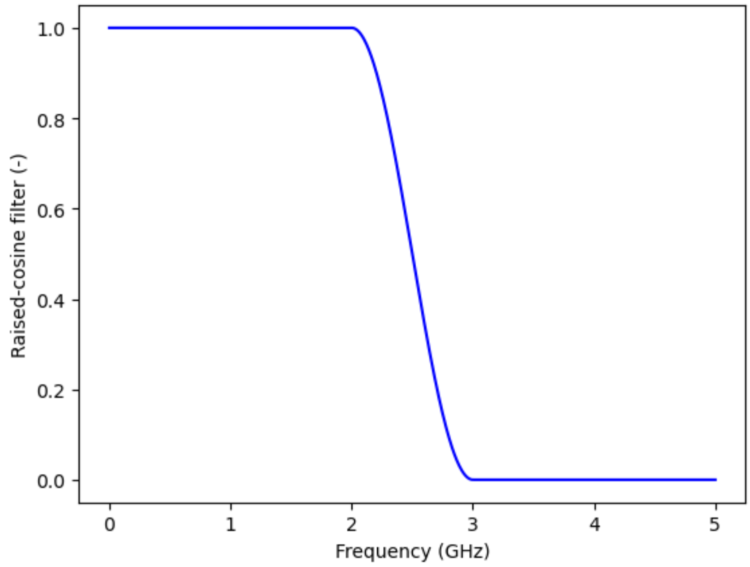

Figure 11: Raised-cosine frequency filter given by Equation (5) with parameters $\omega_0 = 2.5$ GHz and $\beta = 0.2$.

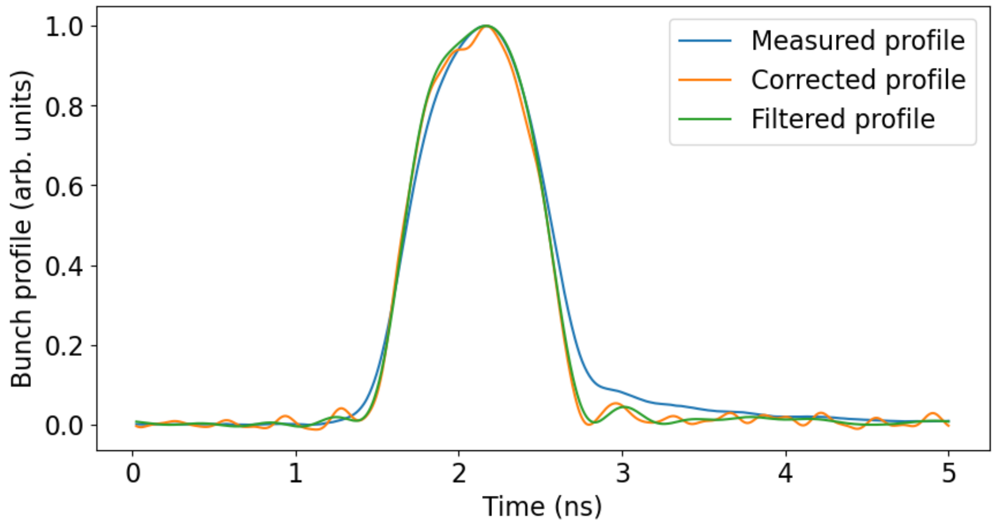

Figure 12: Longitudinal profile of one bunch in experiment B1 at different stages of analysis. **Blue:** the measured profile acquired by the oscilloscope. **Orange:** the corrected profile obtained after applying inverse transfer functions. **Green:** the filtered profile obtained after applying low-pass frequency filter.

4.3 Profile alignment and comparison

After processing the bunch profile data from both instruments, our next goal is to align the profiles in the time domain. To do this, we calculate the cross-correlation function of the profiles measured by the SC and WCM of the same bunch, which is given in Equation (6). Figure 15 shows the profiles measured by the SC and WCM of a bunch from experiment B1 and the calculated cross-correlation between them. We then find the time lag for which the cross-correlation is maximal, Δt, and then displace the WCM profile along the time axis by Δt. The resulting aligned profiles are shown in Figure 16, as well as the magnitude of their spectra in the frequency domain.

Upon alignment, we see that the profiles from each instrument have good agreement, especially along the falling edge of the signal. Along the rising edge, however, the WCM profile displays asym-

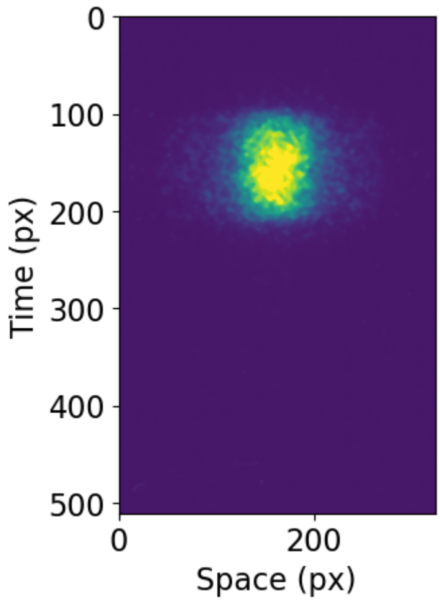

Figure 13: SC image of a bunch from experiment B1 after applying a median filter to remove noisy pixel clusters.

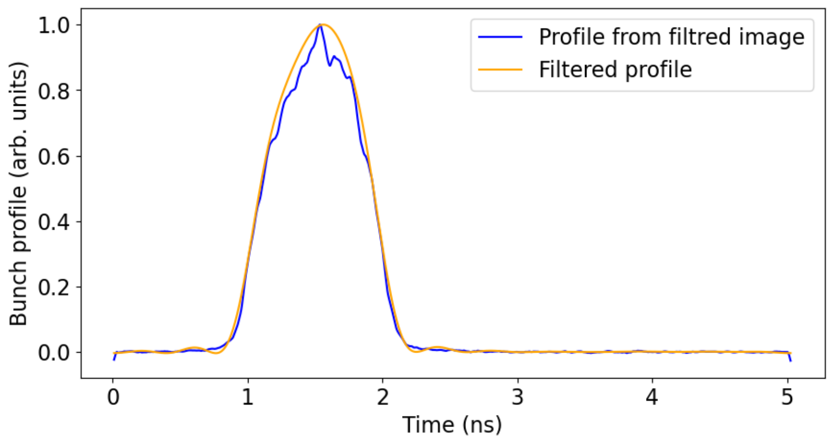

Figure 14: Blue: Profile obtained by projecting median-filtered image onto the time axis. **Orange:** Profile obtained by applying a raised-cosine filter onto the aforementioned profile.

metries close to the signal peak. Additionally, we observe a small yet significant ripple in the signal at around 2.2 ns. It is possible that this is an artifact of the raised-cosine frequency filtering since this ripple is not observed in the SC before applying the filter function (see Figure 14); however, as seen in Figure 12, the WCM profile does contain these ripples before frequency filtering. These findings are consistent across all the acquisitions.

5 Comparison of bunch length measurement techniques

To characterize the bunch length, we first apply a binomial particle distribution fit to the filtered profiles from both the WCM and the SC given by Equation (7). We use a damped least-squares fitting algorithm implemented by the *lmfit* Python library. An example fitting is shown in Figure 17. We observe that the algorithm does a poor job fitting the profiles around the tails; because of this, we do not use the fitted τ parameter to characterize the bunch length.

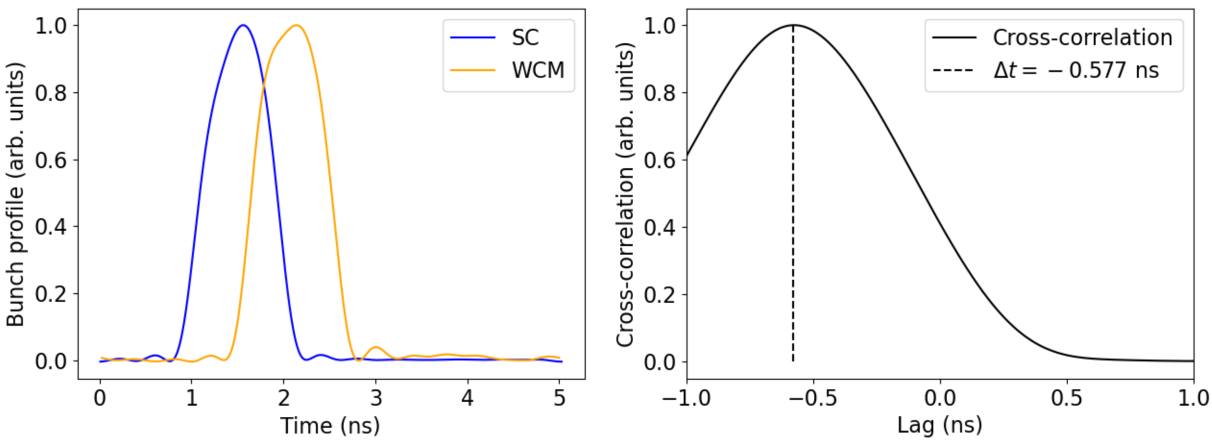

Figure 15: Left: The filtered bunch profile from the SC is shown in blue, and the filtered bunch profile from the WCM is shown in orange. **Right:** The cross-correlation function given by Equation (6), where $x[t]$ is the SC profile and $y[t]$ is the WCM profile. We see that correlation is maximal for a time lag of $\Delta t = -0.577$ ns, as shown in the dotted line.

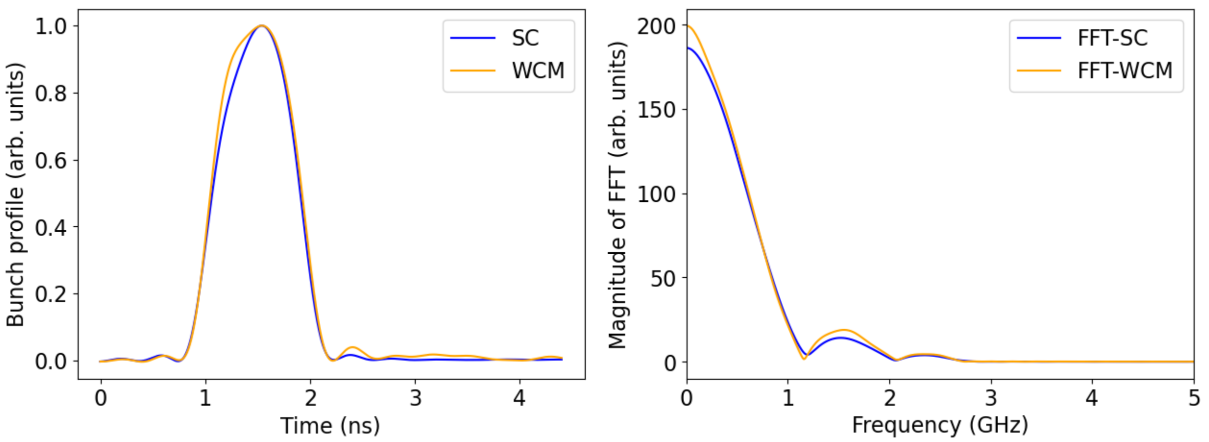

Figure 16: Left: Aligned profiles depicted in Figure 15 using the cross-correlation method of alignment. **Right:** Spectra of both profiles in the frequency domain.

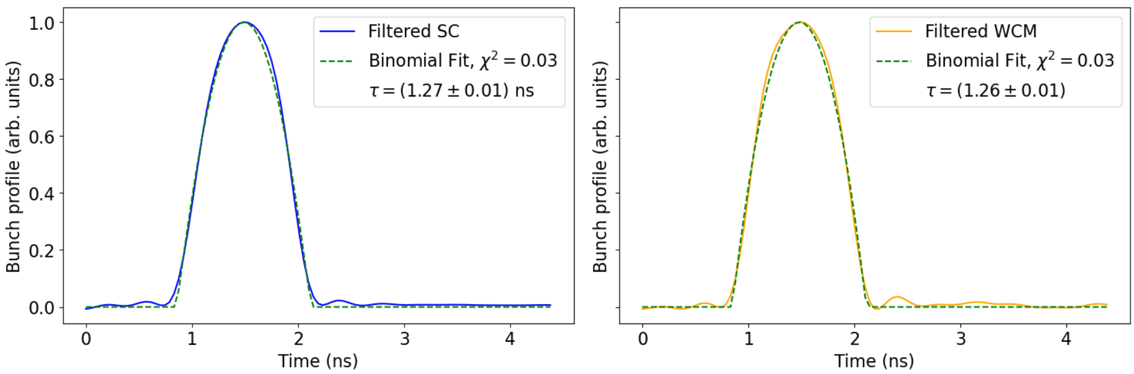

Figure 17: Binomial distribution profile curve fitting of the same bunch from experiment B1. We observe that the fitting algorithm does not do a good job fitting the profile around the tails. **Left:** Curve-fitting of filtered profile from the SC. **Right:** Curve-fitting of filtered profile from the WCM.

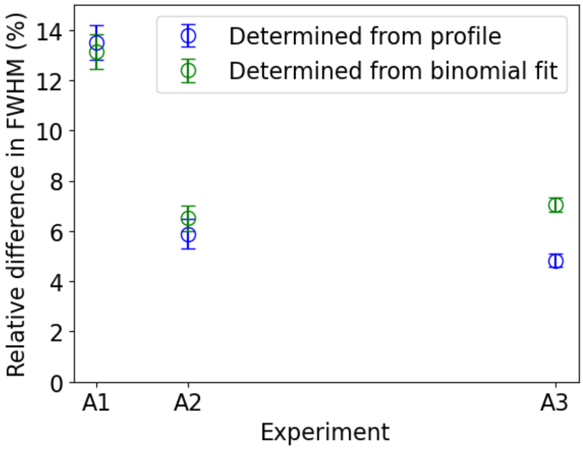

Figure 18: Relative difference in the FWHM between the WCM profile and SC profile (given as a percentage) for experiments with bunch rotation. The axis is oriented where left-to-right shows increasing beam intensity N_p. The relative difference of the FWHM of the filtered profiles is shown in blue, and that of the binomial fit curves is shown in green.

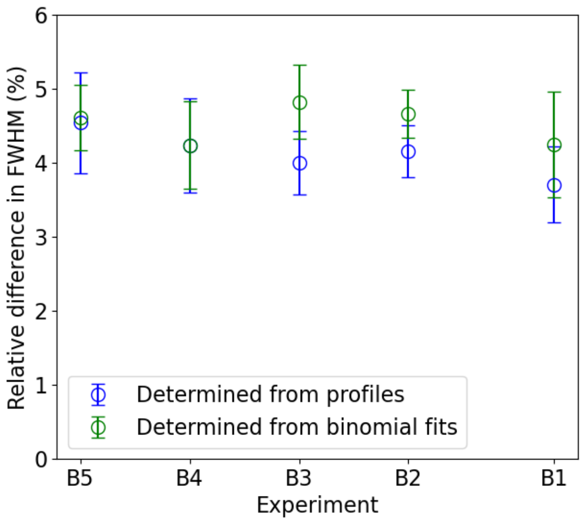

Figure 19: Relative difference in the FWHM between the WCM profile and SC profile (given as a percentage) for experiments without bunch rotation. The axis is oriented where left-to-right shows increasing RF voltage. The relative difference of the FWHM of the filtered profiles is shown in blue, and that of the binomial fit curves is shown in green.

The first observable we investigate is the full-width at half-maximum (FWHM) of each of the profiles as well as the binomial fits of the profiles. For each bunch profile we calculate and average the relative differences in the FWHM given by

$$\text{Relative Difference} = \frac{\text{FWHM}_{\text{WCM}} - \text{FWHM}_{\text{SC}}}{\text{FWHM}_{\text{SC}}} \quad . \tag{8}$$

The results for the experiments with bunch rotation are shown in Figure 18. The results for the experiments without bunch rotation are shown in Figure 19. In both cases, we find that the relative difference is consistently positive, meaning that the WCM measures a longer FWHM of the bunch profile than the SC does.

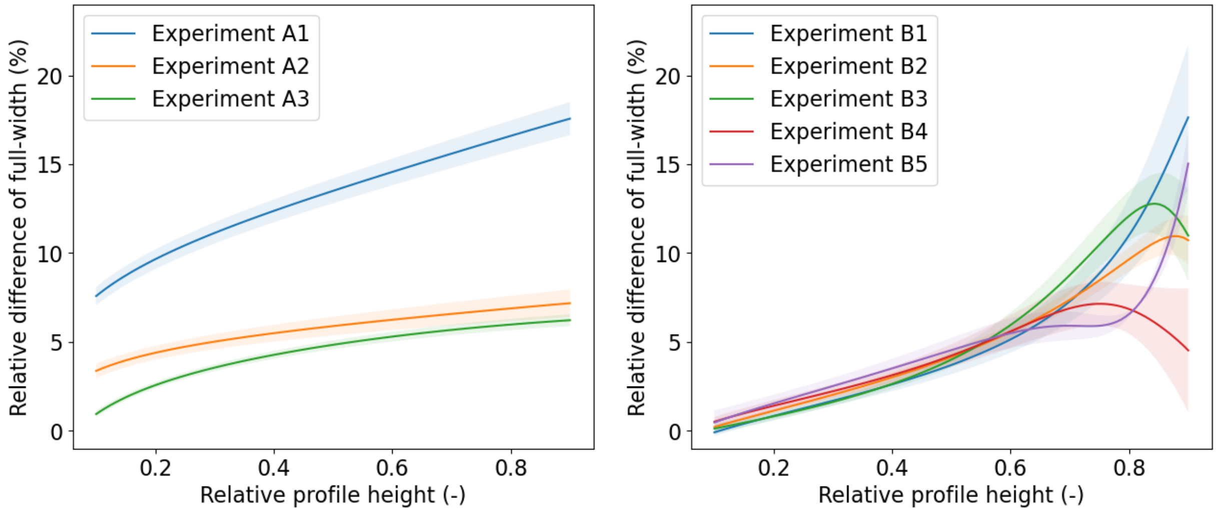

Figure 20: The relative difference in profile width as a function of relative profile height for experiments with bunch rotation (**left**) and without bunch rotation (**right**).

As an additional observable, we look at the relative difference in the profile widths as a function of relative profile height, as shown in Figure 20. For example, a relative profile height of 0.5 would be the FWHM; a relative profile height of 0.1 would be the width of the profile at one-tenth of the maximum. This analysis was done only on the filtered profiles and not the binomial fit curves. Again, we find that the WCM consistently measures a wider profile than the SC does, with a relative difference ranging from 0% to about 21%. We also find that generally, the discrepancy between the profiles from each instrument increases closer to the peak of the profile (that is, at greater relative profile heights). It is yet unclear whether these trends in the discrepancies are in fact due to systematic errors or simply artifacts of our analysis; further work will need to be done to determine this.

6 Estimation of wall current monitor transfer function

Lastly, we can estimate the transfer function of the WCM using Equation (1), where $y[t]$ is the measured bunch profile from the oscilloscope for the WCM, and $x[t]$ is the true profile. For our estimation, we assume the filtered profile from the SC to be the true profile because the SC system has fewer distortions from cabling and electronics. For each bunch in an experiment, we calculate the transfer function by Equation (1), and then we take an average and apply a median filter of size 3 to reduce noise. The results of this calculation for the experiments with bunch rotation are shown in Figure 21. We see agreement between the estimated and measured transfer functions up to about 1.5 GHz. There also appears to be a dependence on the beam intensity; however, this will have to be studied further to confirm. The results for experiments without bunch rotation are shown in Figure 22. Since the bunches in these experiments were significantly longer, the bandwidth of agreement between the measured and estimated transfer functions is noticeably shorter.

7 Conclusions and outlook

In this work, we compared two different techniques for measuring longitudinal bunch profiles based on very distinct mechanisms. The wall current monitor (WCM) detects the bunch signal via coaxial pick-ups, transmitting it to an oscilloscope as an electrical signal through cables and electronics that distort the signal. The Streak Camera (SC) provides higher temporal resolution and dynamic range by converting light emitted from the proton bunch, via optical transition radiation, into a time-resolved image.

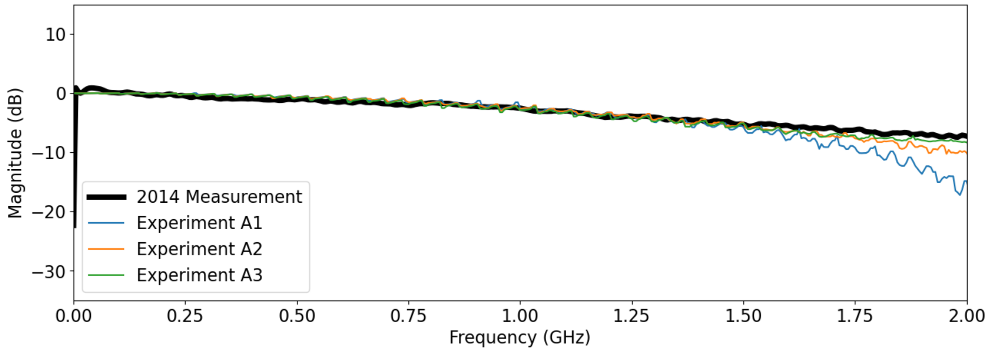

Figure 21: Estimated transfer function using filtered SC profiles from experiments with bunch rotation. In black is the 2014 measurement of the total transfer function from the pick-up (Figure 2) and transfer line (Figure 3).

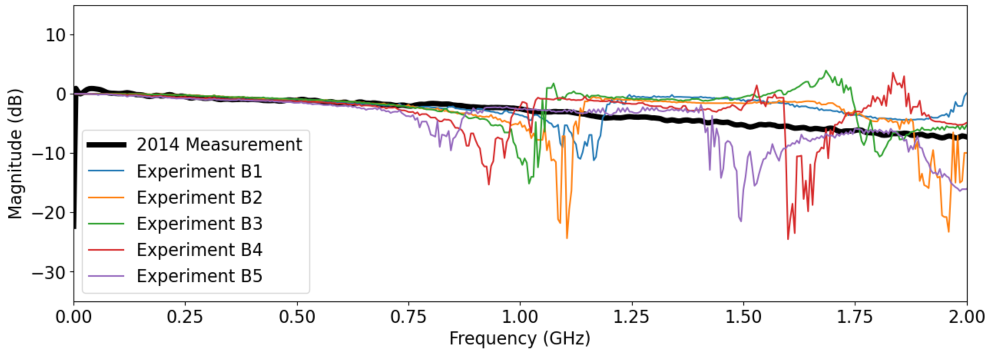

Figure 22: Estimated transfer function using filtered SC profiles from experiments without bunch rotation. As expected, longer bunch lengths result in shorter bandwidth in terms of agreement with the direct measurement.

After retrieving and aligning the corresponding measurements, we applied corrections and filtering to the profiles to make qualitative comparisons between the techniques. Although the agreement is very good, we observed that the WCM measures the bunch profile to be longer than the SC measures by a few percent ($\sim 5\%$).

Additionally, we were able to make an estimate of the total transfer function of the WCM measurement setup by assuming the filtered longitudinal profiles from the SC to be the true profiles. Our estimation was consistent with direct measurements up to around 1.5 GHz; however, this was dependent on the length of the bunches.

A refined measurement of the transfer function has been recently conducted to characterize the WCM pick-up and the cabling transfer function at higher frequencies [5]. Furthermore, we repeated the measurements using a new higher-resolution oscilloscope with a sampling rate of 50 GS/s and 12-bit, but with a different beam type and streak camera used for the HiRadMat experiment. The analysis and results will be presented in a future work.

Acknowledgements

Thanks to the European Organization for Nuclear Research, as well as its partnership with the University of Michigan with support from the National Science Foundation, for providing and funding this amazing opportunity. Additional thanks to my supervisors Leandro Intelisano and Giulia Papotti for their advice and review of this work. Lastly, thanks to the wonderful people at the SY-RF-BR section for teaching and explaining concepts in beam dynamics and for creating a very welcoming atmosphere.

Bibliography

[1] M. Turner and P. Muggli. Understanding time-resolved images of awake proton bunches. (arXiv:2409.18771), September 2024. arXiv:2409.18771 [physics].

[2] Intelisano, Leandro, Heiko Damerau, and Ivan Karpov. 2025. “Threshold for Loss of Landau Damping in Double-Harmonic Rf Systems.” arXiv:2502.14548. Preprint, arXiv, February 21. https://doi.org/10.48550/arXiv.2502.14548.

[3] Bohl, T. & Malo, J. F. (2009) The APWL Wideband Wall Current Monitor

[4] Oguzhan, Kaan, Lucas Ranc, Livio Verra, and Allen Caldwell. 2024. “A Decomposition Algorithm for Streak Camera Data.” arXiv:2401.12269. Preprint, arXiv, January 22. https://doi.org/10.48550/arXiv.2401.12269.

[5] Flowerdew, Jake, Leandro Intelisano, Alexandre Lasheen, and Giulia Papotti. n.d. Cable Transfer Function Measurements and Bunch Length Analysis in the SPS.

[6] Linnecar, Trevor Paul R. 1978. "The high frequency longitudinal and transverse pick-ups used in the SPS." CERN, 1978.

[7] P.K. Hamamatsu, Universal streak camera C10910-05 Catalog, Hamamatsu, Photonics K.k (2022).